



Cite this: *Green Chem.*, 2022, **24**, 8054

Solvent-free photochemical decomposition of sulfur hexafluoride by phosphines: formation of difluorophosphoranes as versatile fluorination reagents†

Philipp Rotering,^{a,b} Christian Mück-Lichtenfeld ^c and Fabian Dielmann ^{a*}

The chemical activation of SF₆ has garnered considerable attention because of its possible utilization as a cheap and safe reagent in chemical synthesis. Such a process becomes particularly attractive when combined with the disposal of the potent greenhouse gas after its technical application. Herein, we report on the photochemical reaction of SF₆ with phosphines, which selectively produces difluorophosphoranes and phosphine sulfides. Computational and experimental studies show that the $\pi(\text{Ar}) \rightarrow \sigma^*(\text{SF}_6)$ charge-transfer excitation of a preformed R₃P...SF₆ complex is the initial activation step. Using triphenylphosphine, the decomposition of SF₆ was carried out in a solvent-free, scalable process, giving a 3:1 mixture of difluorotriphenylphosphorane and triphenylphosphine sulfide (TPP-Fluor), which was utilized for the deoxyfluorination of alcohols and carboxylic acids and for the preparation of common hexafluorophosphate salts.

Received 8th June 2022,
 Accepted 22nd September 2022
 DOI: 10.1039/d2gc02172b
rsc.li/greenchem

Introduction

Sulfur hexafluoride (SF₆) has been recognized as the most potent greenhouse gas among the industrial gases with a global warming potential of 23 500 relative to CO₂ over a 100-year time horizon.¹ It is therefore listed as one of the six greenhouse gases in the 1997 Kyoto Protocol, which implemented regulative measures for SF₆ usage in various industries.² Today, technical uses of SF₆ are largely limited to a few industries, including the electrical industry, which accounts for 80% of SF₆ consumption, and other sectors such as metal casting, semiconductor manufacturing, and medical applications.³ The unique physical and chemical properties of the gas make its use in these areas particularly attractive, sometimes even indispensable.⁴ Despite all efforts to avoid emissions by managing SF₆ in closed cycles or by replacing the greenhouse gas, the concentration of SF₆ in the atmosphere is still on the rise.⁵ The reasons for this trend are diverse, but

related to the fact that the disposal of used SF₆ is challenging due to the extreme chemical inertness of the gas.⁶

The common decomposition process at the end of life of SF₆ in electrical equipment is pyrolysis at temperatures above 1100 °C, whereby the sulfur and fluorine elements are converted to CaSO₄ and CaF₂ by chemical reaction with CaCO₃.⁷ Because this process has high energy requirements and is not suitable for all SF₆ applications, the development of alternative abatement methods is a current field of research.⁸ Particularly worthwhile in this context would be to obtain value-added compounds from the disposal process. Several different approaches exist which we herein divide into two main categories according to the initial activation strategy.

The first class of methods involves the direct fragmentation of SF₆ under forcing conditions, *e.g.*, *via* pyrolysis, photolysis or by various plasma methods.⁸ Since the inertness of SF₆ arises from kinetic barriers to dissociation rather than its high thermodynamic stability, a clear advantage of the direct fragmentation strategy is that cheap reactants such as CaCO₃, H₂S, H₂O or O₂ can be applied to capture the SF₆ fragments and no additional reagents or solvents are required. Notably, the use of catalysts can significantly alleviate the harsh conditions, but is associated with additional costs for catalyst replacement.⁹ The decomposition products are usually toxic and corrosive and require appropriate secondary treatment before they can be released. Moreover, the utilization of the decomposition products in fluorinations is hampered by the extreme reaction conditions and the low selectivity of the methods.

^aInstitute of General, Inorganic and Theoretical Chemistry, Leopold-Franzens-Universität Innsbruck, Inrain 80-82, 6020 Innsbruck, Austria.

E-mail: fabian.dielmann@uibk.ac.at

^bInstitut für Anorganische und Analytische Chemie, Westfälische Wilhelms-Universität Münster Correnstrasse 30, 48149 Münster, Germany

^cOrganisch-Chemisches Institut, Westfälische Wilhelms-Universität Münster Corrensstrasse 40, 48149 Münster, Germany

† Electronic supplementary information (ESI) available. See DOI: <https://doi.org/10.1039/d2gc02172b>



In the second class of methods, SF_6 is chemically activated in solution under mild conditions, which involves a single-electron transfer or the nucleophilic attack on SF_6 and therefore requires strongly reducing or highly nucleophilic substances, respectively. Compounds that react with SF_6 at ambient conditions include alkali metals in liquid ammonia,¹⁰ strong organic reductants,^{11–13} electron-rich phosphines,¹⁴ N-heterocyclic carbenes,^{15,16} reactive anions,^{17,18} aluminium(i) compounds,¹⁹ transition metal complexes^{20–22} and organic radicals generated photolytically.²³ These transformations are often highly selective and afford well-defined products which can be considered as potential fluorination agents.^{11,13,15,18,22} A disadvantage, however, is the need to conduct the reaction under inert gas due to the high reactivity of the reductants. A milestone towards the use of less sensitive and easier to handle stoichiometric reducing agents was the rhodium-catalyzed degradation of SF_6 using silanes as reducing agents and phosphines as sulfur scavenger.²⁰ Using photosensitizers for the reductive activation of SF_6 , the reaction was carried out in the presence of suitable substrates, which enabled deoxyfluorination of alcohols and pentafluorosulfanation of styrene derivatives.^{24–27} Despite the promising achievements in using SF_6 as a fluorination reagent, when it comes to the disposal of surplus SF_6 on a large scale in a cost-effective manner, these solution-phase strategies have the drawback of requiring expensive reagents, catalysts, and hazardous organic solvents. Although only carried out on a small scale, the electrochemical reduction of SF_6 has the potential to overcome some of these drawbacks.²⁸ Given these considerations, our intention was to combine the advantages of both categories and develop a solvent-free process that would yield well-defined products which could be used as fluorination reagents in chemical synthesis.

We have recently shown that the electron-releasing character of phosphines is significantly enhanced by attaching strong π -donor substituents to the phosphorus atom.²⁹ Phosphines equipped with three substituents are ranked among the strongest nonionic superbases and are characterized by extreme reactivity towards electrophiles.³⁰ Accordingly, unlike commercially available alkyl or aryl phosphines, phosphines modified in this way can activate SF_6 at ambient conditions and convert it into potential fluorinating reagents.¹⁴ The recent report by Braun and coworkers on the photochemical activation of SF_6 by N-heterocyclic carbenes inspired us to consider the reaction of more simple phosphines with SF_6 triggered by irradiation with light, which we report herein.¹⁵

Results and discussion

Among commercially available phosphines, triphenylphosphine has the most attractive properties for a scalable degradation of SF_6 because it is an inexpensive, nontoxic, air-stable solid that is produced on a large scale. However, as demonstrated previously, Ph_3P is not nucleophilic enough to activate SF_6 even at elevated temperature.¹⁴ To investigate

whether light can induce the reaction, we first recorded the UV-vis spectra of Ph_3P in THF under an atmosphere of argon or SF_6 . Both spectra were identical and only showed an absorption band at 240–310 nm (Fig. 1). Previous studies on the photolysis of Ph_3P showed that this absorption involves the $\text{n} \rightarrow \pi^*$ excitation leading to the homolytic cleavage of a P–Ph bond.^{31,32} We therefore irradiated 0.2 M solutions of Ph_3P in THF under an atmosphere of 1 bar SF_6 using narrow-band LED light sources (see the SI for details). Exposure of the solution to UV light at 310 nm gave several P–F species, including Ph_4P^+ and Ph_2PF_3 , in agreement with the photolytic cleavage of P–Ph bonds. However, the formation of P–F species likewise indicates the successful activation of SF_6 under these conditions. Irradiation of the solution with light at 365 nm or 405 nm led to the clean conversion of Ph_3P into a 3 : 1 mixture of difluorotriphenylphosphorane and triphenylphosphine sulfide within 6 hours or 16 hours, respectively. Note that the reaction is significantly faster using light at 365 nm, despite the lower relative irradiance (365 nm LED: 9 mW cm^{-2} , 405 nm LED: 28 mW cm^{-2}). No reaction between Ph_3P and SF_6 was observed with blue (450 nm) or orange (585 nm) light.

We next irradiated solid Ph_3P under an SF_6 atmosphere for 24 hours using the 365 nm LEDs. Although the solid material turned light brown at the solid–gas interface facing the light source, the ^{31}P and ^{19}F NMR spectra of the dissolved solid product revealed that less than 1% of the Ph_3P had been converted to fluorinated species. We then carried out the photo-reaction using a Ph_3P melt to increase the direct contact between the reactants. Irradiation of a Ph_3P melt at 80 °C under 1 bar SF_6 atmosphere resulted in the quantitative formation of difluorotriphenylphosphorane and triphenylphosphine sulfide in a ratio of 3 : 1 within 8 hours (Scheme 1). The difluorophosphorane can be separated from the phosphine sulfide by recrystallization from α,α,α -trifluorotoluene in 81% yield. However, separation of the products proved unnecessary for applications of Ph_3PF_2 in fluorination reactions owing to the chemical inertness of Ph_3PS (*vide infra*). The

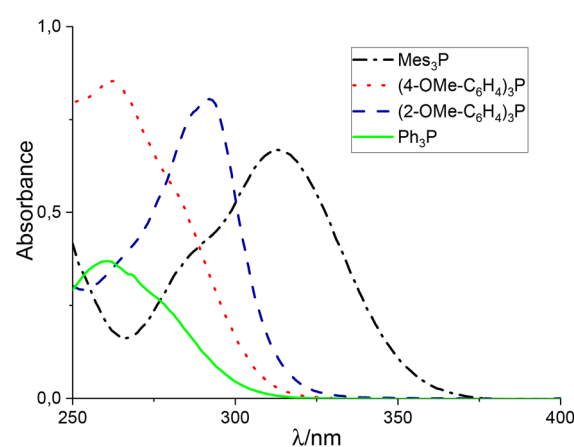
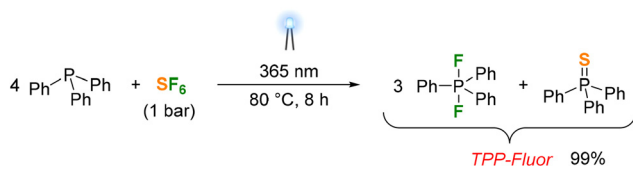


Fig. 1 Experimental UV-vis spectra of selected triarylphosphines ($c = 3.8 \times 10^{-5}$ M in THF).





Reaction characteristics:

- PPh_3 is a non-toxic, air-stable, solid bulk chemical
- solvent-free, scalable process
- quantitative conversion to solid products
- generation of a fluorination reagent

Scheme 1 Photoreduction of SF_6 with triphenylphosphine affording a 3:1 mixture of difluorotriphenylphosphorane and triphenylphosphine sulfide.

obtained 3:1 mixture of Ph_3PF_2 and Ph_3PS is therefore referred to as TPP-Fluor in the following. To demonstrate the scalability of the process, a flat-bottomed glass vessel containing 100 g of Ph_3P under 1 bar SF_6 pressure was placed above an LED array (see the ESI for details†). Upon irradiation with light at 365 nm, Ph_3P started to melt in the vessel due to heat uptake from the LED array, producing TPP-Fluor within 9 hours in quantitative yield. It is noteworthy that the reaction time increases only slightly despite the tenfold scale of the reaction, suggesting that the reaction rate is limited by the solubility and diffusion of SF_6 in Ph_3P .

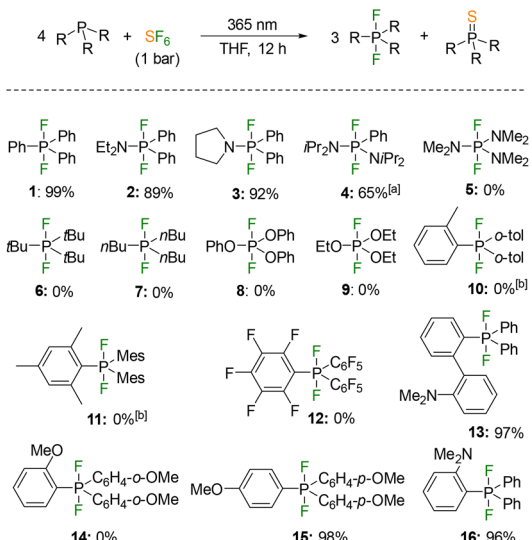
The scope of the photochemical reaction between phosphines and SF_6 was investigated by irradiating THF solutions of various phosphines under 1 bar SF_6 atmosphere with light at 365 nm (Scheme 2). Several phosphines were smoothly converted into the difluorophosphorane derivatives in excellent yield, while other phosphines did not react with SF_6 under

these conditions. While this behaviour can be rationalized by the electron-poor character of perfluorinated phosphines (12) and phosphites (8, 9), it is unexpected for the alkylphosphines and aminophosphines (5–7), because they are stronger reducing agents than triphenylphosphine. In addition, electron-rich arylphosphines were readily converted into the difluorophosphoranes (13, 15, 16). An explanation for this behaviour can be derived from the series of aminophosphines (2–5), which show a trend of decreasing reactivity with the number of phenyl groups and suggests that the photochemical reaction with SF_6 requires at least one phenyl group at the phosphorus atom. Finally, *ortho* substituents appear to hamper the reaction (14) or lead to decomposition reactions (10, 11). Note that the decomposition of the sterically more encumbered phosphines (10, 11) was also observed upon irradiation with light at 365 nm in the absence of SF_6 and is attributed to the red-shifted $n(\text{P}) \rightarrow \pi^*(\text{Mes})$ absorption band (Fig. 1).

Previous studies showed that the photoexcitation of Ph_3P with light at $\lambda = 266$ nm leads to the homolytic cleavage of a phosphorus-phenyl bond to form the diphenylphosphinyl radical $\text{Ph}_2\text{P}^\bullet$ and phenyl radical Ph^\bullet .^{31–34} This P–C bond cleavage has been reported to occur either from the singlet ($^1\text{Ph}_3\text{P}^*$) or the triplet excited state ($^3\text{Ph}_3\text{P}^*$).^{33,34} However, when Ph_3P is irradiated in the presence of molecular oxygen, an electron transfer to O_2 occurs from the photoexcited state of Ph_3P to give the radical ion pair $\text{Ph}_3\text{P}^{+}/\text{O}_2^{\bullet-}$.³⁵ The reaction produces triphenylphosphine oxide in excellent yield upon irradiation with light of wavelengths over 310 nm. However, very sluggish oxidation of Ph_3P was observed using light with longer wavelength than 350 nm. By contrast, the reaction between Ph_3P and SF_6 is triggered by light of $\lambda > 350$ nm and produces only products with intact P–Ph bonds. We therefore consider an initial $n(\text{P}) \rightarrow \pi^*$ excitation of Ph_3P followed by subsequent electron transfer to SF_6 unlikely, especially since no decomposition of Ph_3P with light at 365 nm or 405 nm was observed in the absence of SF_6 (Fig. S58†).

To gain an insight into the reaction pathway of arylphosphines with SF_6 focussing on the initial activation step, we performed DFT calculations at the PW6B95-D3//TPSS-D3/def2-TZVP level of theory using the COSMO-RS solvation model with THF for 298 K (see the ESI†). The proposed mechanism for the formation of Ph_3PF_2 from Ph_3P and SF_6 is illustrated in Fig. 2. Starting from an endergonic encounter complex $[\text{Ph}_3\text{P} \cdots \text{SF}_6]$, electronic excitation occurs with a calculated wavelength of 360 nm (step A in Fig. 2) and corresponds to a charge-transfer state in which one electron is transferred from a π orbital of the arene (HOMO–1, Fig. 4a) to the delocalized σ^* orbital of SF_6 (LUMO, Fig. 4b). According to the TD-DFT result, the $n(\text{P}) \rightarrow \sigma^*(\text{SF}_6)$ transition occurs at a higher wavelength (525 nm) with low oscillator strength, and thus it is not expected to be involved in the reaction (Fig. 3). This conclusion agrees with the experimental observation that light at 585 nm does not induce the photochemical reaction and that phosphines lacking aryl substituents do not react with SF_6 .

To get a qualitative insight into the photochemical processes that may occur after the charge transfer excitation, we



Scheme 2 Scope of the photochemical activation of SF_6 by phosphines affording a mixture of phosphine sulfides and difluorophosphoranes, of which only the latter are depicted. Yields determined by ^{31}P NMR spectroscopy. ^aPhosphine present in reaction mixture. ^bDecomposition of the phosphine upon irradiation.



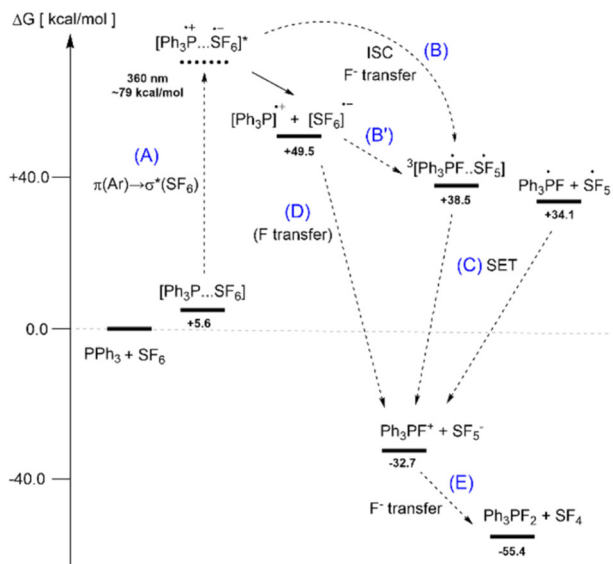


Fig. 2 Energy diagram of the proposed mechanism for the photochemical reaction of Ph_3P with SF_6 . ΔG : PW6B95-D3/TPSS-D3/def2-TZVP + COSMO-RS(THF). TDDFT: B3LYP/def2-TZVP + CPCM(THF). Free energies are reported with respect to isolated Ph_3P and SF_6 and include implicit solvation energies in THF.

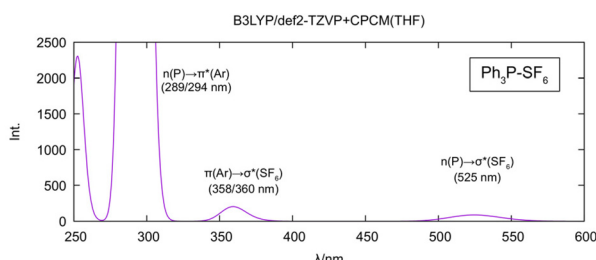


Fig. 3 Calculated absorption spectrum of $[\text{Ph}_3\text{P}\cdots\text{SF}_6]$ using TD-DFT at the B3LYP/def2-TZVP level of theory and the implicit solvation model CPCM(THF).

have located the conical intersection that connects the S_0 and S^* state of the complex using the range-separated hybrid functional CAM-B3LYP³⁶ and the def2-SVP basis set.³⁷ In the ionic complex, the distance between the two ions ($d(\text{P}\cdots\text{S}) = 3.74 \text{ \AA}$) is significantly smaller than in the ground state complex ($d(\text{P}\cdots\text{S}) = 4.81 \text{ \AA}$), while the SF bonds are elongated by about 0.07 \AA . This indicates that the charge-transfer excitation promotes the reaction by driving the reactants to a distance short enough for electron and/or fluorine transfer.

In agreement with this observation, we were not able to locate a transition structure for F transfer with our (ground state) DFT calculations. Only when we optimized the triplet state of the complex (${}^3[\text{Ph}_3\text{P}\cdots\text{SF}_6]$), which could be formed by intersystem crossing from the charge transfer state (S^*), we observed immediate fluoride ion transfer to give the radical ion pair ${}^3[\text{Ph}_3\text{PF}\cdots\text{SF}_5]$ (step **B**). Therein, the spin density is evenly distributed over both fragments of the triplet complex

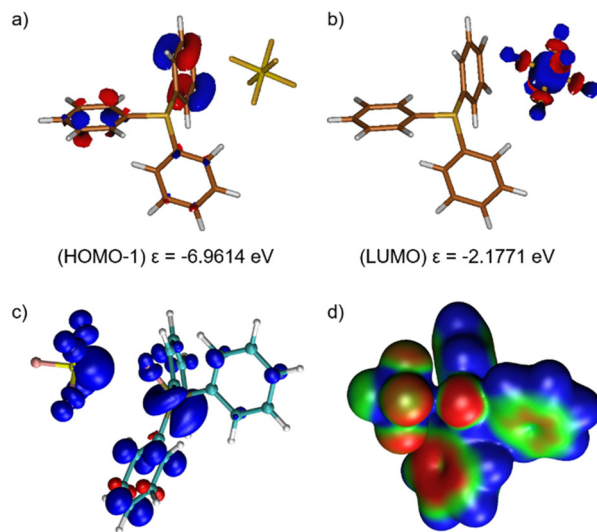


Fig. 4 (a and b) Frontier orbitals of the encounter complex $[\text{Ph}_3\text{P}\cdots\text{SF}_6]$. Orbital energies calculated with B3LYP/def2-TZVP + CPCM(THF). Isosurface value 0.05 a.u. (c) Spin density $\rho_\alpha - \rho_\beta$ (isosurface value = 0.005 a.u.) and (d) electrostatic potential (isodensity value 0.02 a.u.) of the optimized triplet state ${}^3[\text{Ph}_3\text{PF}\cdots\text{SF}_5]$ (PW6B95//TPSS-D3/def2-TZVP).

(Fig. 4c), and the unpaired electron in $(\text{Ph}_3\text{PF})^*$ occupies the σ^* orbital of the P-F bond, partially delocalized in one phenyl ring. The radical ion pair ${}^3[\text{Ph}_3\text{PF}\cdots\text{SF}_5]$ can either dissociate or instantaneously transfer an electron after ISC to form the ion pair $[\text{Ph}_3\text{PF}]^+/\text{[SF}_5]^-$ (step **C**). Note that the radical ion pair $[\text{Ph}_3\text{P}]^{++}/\text{[SF}_6]^{--}$ representing the “dissociated” charge-transfer state, has a relative free energy of $49.5 \text{ kcal mol}^{-1}$, which is well below the photoexcited state. We therefore cannot distinguish whether a consecutive fluoride (**B/B'**) and electron transfer (**C**) or a direct fluorine atom transfer (**D**) occurs after photoexcitation. These processes are presumably fast and involve closely associated ion pairs. Overall, the first reaction step is exergonic ($-32.7 \text{ kcal mol}^{-1}$) and involves a formal “ F^+ transfer” resulting in the ion pair $[\text{Ph}_3\text{PF}]^+/\text{[SF}_5]^-$, which is strongly stabilized by solvation in THF. The subsequent fluoride transfer (step **E**) is exergonic by more than $-20 \text{ kcal mol}^{-1}$ and expected to have a low energy barrier.¹⁴

The UV-vis spectra of the free phosphines Ph_3P , Mes_3P , $(2\text{-OMe-C}_6\text{H}_4)_3\text{P}$, $(4\text{-OMe-C}_6\text{H}_4)_3\text{P}$ and of the corresponding noncovalent SF_6 complexes were calculated using TD-DFT at the B3LYP/def2-TZVP level of theory and the implicit solvation model CPCM for THF. The free phosphines exhibit a strong absorption band of the $n(\text{P}) \rightarrow \pi^*(\text{Ar})$ excitation (Fig. S63†). In agreement with the experimental spectra (Fig. 1), the absorption band appears at 290 nm for Ph_3P and is blue-shifted for $(4\text{-OMe-C}_6\text{H}_4)_3\text{P}$, but red-shifted for the arylphosphines with substituted *ortho* positions. The $n \rightarrow \pi^*$ excitation of Mes_3P covers the region of irradiation (365 nm), which explains the observed decomposition reaction. Although we tend to be cautious with the interpretation of the excitation spectra obtained with the hybrid functional B3LYP, a comparison of the UV

region of the noncovalent SF_6 complexes is qualitatively in good agreement with the experimental observations (Fig. S64†): only $[\text{Ph}_3\text{P}\cdots\text{SF}_6]$ and $[(4\text{-OMe-C}_6\text{H}_4)_3\text{P}\cdots\text{SF}_6]$ absorb with significant intensity at 365 nm due to the $\pi(\text{Ar}) \rightarrow \sigma^*(\text{SF}_6)$ charge transfer excitation. The *ortho*-substituted aryl phosphines either have a different absorption maximum ($(2\text{-OMe-C}_6\text{H}_4)_3\text{P}$: 385 nm), or the $n(\text{P}) \rightarrow \pi^*(\text{Ar})$ band is extended into the region of the charge-transfer excitation (Mes_3P). Irradiation of THF solutions of Mes_3P , $(o\text{-tol})_3\text{P}$ or $(2\text{-OMe-C}_6\text{H}_4)_3\text{P}$ for 3 hours under an SF_6 atmosphere with light at 405 nm did not cause the phosphines to decompose or react with SF_6 . For Mes_3P , this is consistent with the computational results. However, the lack of reactivity in the case of $(2\text{-OMe-C}_6\text{H}_4)_3\text{P}$ suggests that the steric bulk of the phosphine preventing the formation of the encounter complex must also be considered.

Since our experimental and computational results suggest that the initial SF_6 activation step corresponds to a $\pi(\text{Ar}) \rightarrow \sigma^*(\text{SF}_6)$ charge transfer excitation, we further investigated the versatility of our approach by using an external π system as photosensitizer combined with an alkyl phosphine as reductant. Tri-*n*-butylphosphine does not react with SF_6 upon irradiation with light at 365 nm (*cf.* Scheme 2). However, when the reaction is performed in the presence of stoichiometric amounts of benzophenone or acetophenone as photosensitizer, $(n\text{Bu})_3\text{P}$ reacts with SF_6 within 24 h to give a mixture of tri-*n*-butylphosphine sulfide and tri-*n*-butyldifluorophosphorane (Scheme 3). The reaction is more selective with acetophenone than with benzophenone. With catalytic amounts of the photosensitizer (20 mol%), the reaction rate is significantly lower (Table S1†). No reaction with SF_6 was observed when THF solutions of triethyl phosphite or triphenyl phosphite were irradiated under the same conditions using acetophenone as photosensitizer.

Collectively, the photochemical reaction of SF_6 with phosphines proves to be general enough to afford alkyl-, aryl-, and heteroaryl-substituted phosphine sulphides and difluorophosphoranes. The latter are important starting materials in the context of Lewis acid-catalyzed transformations³⁸ or CO_2 sequestration.³⁹ They are usually synthesized by oxidation of the phosphines using harsh reagents such as XeF_2 , SF_4 , HgF_2 or N_2F_4 ,⁴⁰ but more convenient protocols have been recently developed.⁴¹

Owing to the straight-forward synthetic access, the utilization of TPP-Fluor as reagent in chemical synthesis is particularly interesting in terms of a chemical valorization of SF_6 after its technical application. In fact, difluorotriphenylphosphor-

ane has been successfully applied as deoxyfluorination reagent to convert primary and secondary alcohols into fluoroalkanes at reaction temperatures above 140 °C.⁴² As a proof of principle, the deoxyfluorination of 1-hexanol was performed with the TPP-Fluor reagent and gave 1-fluorohexane in 22% yield. We also used TPP-Fluor for the preparation of acyl fluorides directly from carboxylic acids. Acyl fluorides are versatile reagents in chemical synthesis that can be prepared from carboxylic acids using cyanuric fluoride,⁴³ BrF_3 ,⁴⁴ SeF_4 ,⁴⁵ $(\text{Me}_4\text{N})\text{SCF}_3$ ⁴⁶ or sulfur-based fluorination reagents.⁴⁷ Recently, Prakash and co-workers disclosed a protocol for the stepwise conversion of carboxylic acids into acyl fluorides using $\text{Ph}_3\text{P}/\text{NBS}$ for the activation of the carboxylic acid and $\text{Et}_3\text{N}\text{-3HF}$ as fluoride ion source.⁴⁸

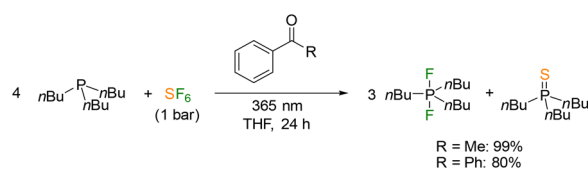
Lauric acid was selected as model substrate to optimize the reaction conditions (Table 1). The progress of the deoxyfluorination was monitored by ^{31}P and ^{19}F NMR spectroscopy, confirming the formation of Ph_3PO , lauroyl fluoride and HF/FHF^- . We suspect that the liberation of HF during the reaction is the reason why three equivalents of difluorophosphorane (1 eq. TPP-Fluor) are required to achieve good conversion (Table 1, entries 1–4), albeit the addition of 2,6-lutidinium triflate as proton source had little influence on the yield (Table 1, entry 7). The reaction was inhibited under Brønsted basic conditions by using sodium carboxylate as substrate or by adding CsF as an additional nucleophile (Table 1, entries 6 and 8).

Application of the optimized conditions to the deoxyfluorination of various carboxylic acids illustrates its synthetic capabilities (Scheme 4). Aliphatic carboxylic (**17**, **19**, **20**) acids were readily converted to the corresponding products independent of the steric bulk of the alkyl group. Among the aromatic carboxylic acids only the electron-rich benzoic acids (**22**, **23**) underwent the desired transformation, while the reaction is sluggish for benzoic acids bearing electron-neutral (**18**, **21**) or electron-withdrawing functionalities (**25**, **26**). Ester functions (**24**) were not tolerated because the liberated HF/FHF^- cleaves the ester bond, concomitant with further deoxyfluorinations.

Table 1 Optimization of the reaction conditions for the deoxyfluorination of lauric acid using TPP-Fluor

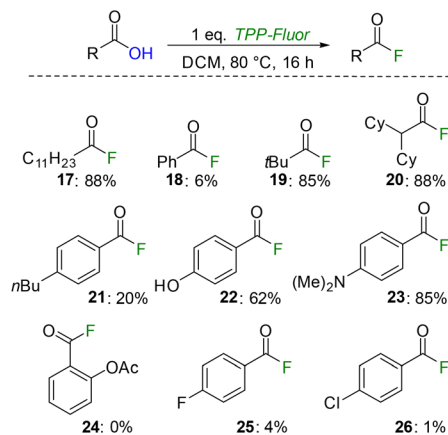
Entry	Conditions	R	Additive	TPP-Fluor (equiv.)	Yield ^a (%)
1	80 °C, 16 h	H	—	0.17	21
2	80 °C, 16 h	H	—	0.33	36
3	80 °C, 16 h	H	—	0.66	69
4	80 °C, 16 h	H	—	1	88
5	60 °C, 16 h	H	—	1	19
6	80 °C, 16 h	H	2 CsF	0.33	<5
7	80 °C, 16 h	H	2 Lut·HOTFF	0.33	44
8	80 °C, 16 h	Na	—	1	<5

^a As determined by quantitative ^{19}F NMR spectroscopy using α,α,α -trifluorotoluene as internal standard.



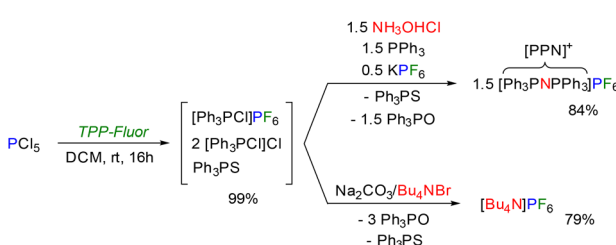
Scheme 3 Photochemical reaction of SF_6 with an alkylphosphine using photosensitizers.





Scheme 4 Direct deoxyfluorination of carboxylic acids using TPP-Fluor. Yields determined by quantitative ^{19}F NMR spectroscopy using α,α,α -trifluorotoluene as internal standard.

We also considered using TPP-Fluor for the fluorination of inorganic substrates (Scheme 5). Treatment of phosphorus pentachloride with TPP-Fluor resulted in complete exchange of fluoride and chloride atoms to give a mixture of chlorotriphenylphosphonium chloride and hexafluorophosphate salts. As already observed in the deoxyfluorination reactions, Ph_3PS did not participate in the reaction. The hexafluorophosphate ion can be readily precipitated from the mixture in good yield as Bu_4NPF_6 after aqueous workup and addition of Bu_4NBr . Furthermore, $[\text{PPN}]^+\text{PF}_6^-$ was assembled from the chlorotriphenylphosphonium ions following the $[\text{PPN}]^+$ cation synthesis of Ruff and Schlientz by treating the reaction mixture with hydroxylamine hydrochloride and additional Ph_3P .⁴⁹ Both reactions demonstrate novel, straightforward routes to salts consisting of weakly coordinating ions, of which Bu_4NPF_6 is a common electrolyte in electrochemistry. It is noteworthy that chlorotriphenyl-phosphonium salts are the key intermediates in the large-scale industrial recycling process of triphenylphosphine oxide, which is based on the chlorination of Ph_3PO with phosgene and subsequent reduction with aluminium powder.⁵⁰ Moreover, there are several elegant methods for the recycling of Ph_3PO and Ph_3PS to Ph_3P ,⁵¹ including electrochemical methods^{50,52} and methods based on the use of dihydrogen gas as reducing agent.⁵³



Scheme 5 Direct conversion of PCl_5 into PF_6^- salts using TPP-Fluor. Isolated yields are reported.

Conclusions

In conclusion, this report discloses a user-friendly, scalable protocol for the photochemical degradation of SF_6 . The solvent-free process produces a well-defined solid fluorinating reagent consisting of a 3:1 mixture of difluorotriphenylphosphorane and triphenylphosphine sulfide, referred to as TPP-Fluor. Utilization of TPP-Fluor for the deoxyfluorination of alcohols and carboxylic acids and for the preparation of common hexafluorophosphate salts from PCl_5 was established. Both reactions highlight possibilities to generate value-added products from the decomposition of the greenhouse gas SF_6 after its technical application by using inexpensive commodity chemicals.

The photochemical reaction between phosphines and SF_6 can also be performed in solution providing a convenient approach to various difluorophosphoranes without the need for hazardous fluorination reagents. Reaction screening with phosphines bearing different substitution patterns revealed that at least one aryl substituent is required for the photochemical SF_6 activation. Alternatively, acetophenone can be used as photosensitizer to drive the fragmentation of SF_6 with alkyl phosphines. Computational studies indicate that the reaction proceeds through a $\pi(\text{Ar}) \rightarrow \sigma^*(\text{SF}_6)$ charge-transfer excitation as the initial activation step, followed by a fluorine/electron or a direct fluoride transfer. While it is generally assumed that the photochemical activation of SF_6 occurs *via* excitation of the reductant, which then facilitates the electron transfer to SF_6 ,^{15,24-27} our study suggests that direct charge-transfer excitation of a preformed SF_6 complex must also be considered. This result implies that substances susceptible to decomposition upon irradiation with short wavelength light can still react with SF_6 upon charge-transfer excitation by light with a longer wavelength and thus opens new avenues for the photochemical derivatization of SF_6 , which is under current investigation in our laboratory.

Author contributions

P. R. carried out the synthetic experiments and analysed the experimental data. C. M.-L. performed the computational investigations. F. D., P. R. and C. M.-L. wrote the manuscript. F. D. directed the investigations.

Conflicts of interest

There are no conflicts to declare.

Acknowledgements

The authors gratefully acknowledge financial support from the DFG (Emmy Noether program: DI 2054/1-1, SFB 858). We thank DILO GmbH for the generous donation of SF_6 gas and Jonas Franzen for helping with experiments for the revision.



References

1 Ø. Hodnebrog, M. Etminan, J. S. Fuglestvedt, G. Marston, G. Myhre, C. J. Nielsen, K. P. Shine and T. J. Wallington, *Rev. Geophys.*, 2013, **51**, 300–378.

2 C. Breidenich, D. Magraw, A. Rowley and J. W. Rubin, *Am. J. Int. Law.*, 1998, **92**, 315–331.

3 (a) B. K. Sovacool, S. Griffiths, J. Kim and M. Bazilian, *Renewable Sustainable Energy Rev.*, 2021, **141**, 110759; (b) C. T. Dervos and P. Vassiliou, *J. Air Waste Manage. Assoc.*, 2000, **50**, 137–141.

4 (a) M. Rabie and C. M. Franck, *Environ. Sci. Technol.*, 2018, **52**, 369–380; (b) P. Billen, B. Maes, M. Larrain and J. Braet, *Energies*, 2020, **13**, 1807.

5 (a) ESRL Global Monitoring Laboratory, *Halocarbons and other Atmospheric Trace Species, Sulfur hexafluoride (SF₆) – Combined Data Set*, 2021, Available: <https://www.esrl.noaa.gov/gmd/hats/combined/SF6.html>; (b) P. G. Simmonds, M. Rigby, A. J. Manning, S. Park, K. M. Stanley, A. McCulloch, S. Henne, F. Graziosi, M. Maione, J. Arduini, S. Reimann, M. K. Vollmer, J. Mühle, S. O'Doherty, D. Young, P. B. Krummel, P. J. Fraser, R. F. Weiss, P. K. Salameh, C. M. Harth, M.-K. Park, H. Park, T. Arnold, C. Rennick, L. P. Steele, B. Mitrevski, R. H. J. Wang and R. G. Prinn, *Atmos. Chem. Phys.*, 2020, **20**, 7271–7290.

6 (a) J. R. Case and F. Nyman, *Nature*, 1962, **193**, 473; (b) K. Seppelt, *Chem. Rev.*, 2015, **115**, 1296–1306.

7 G. Mauthe, L. Niemeyer, B. M. Pryor, R. Probst, H. Bräutigam, P. A. O'Connell, K. Pettersson, H. D. Morrison, J. Poblotzki and D. Koenig, *Electra*, 1996, **164**, 121–131.

8 X. Zhang, H. Xiao, J. Tang, Z. Cui and Y. Zhang, *Crit. Rev. Environ. Sci. Technol.*, 2017, **47**, 1763–1782.

9 (a) J. Zhang, J. Z. Zhou, Z. P. Xu, Y. Li, T. Cao, J. Zhao, X. Ruan, Q. Liu and G. Qian, *Environ. Sci. Technol.*, 2014, **48**, 599–606; (b) J. Zhang, J. Z. Zhou, Q. Liu, G. Qian and Z. P. Xu, *Environ. Sci. Technol.*, 2013, **47**, 6493–6499; (c) N.-K. Park, H.-G. Park, T. J. Lee, W.-C. Chang and W.-T. Kwon, *Catal. Today*, 2012, **185**, 247–252; (d) D. Kashiwagi, A. Takai, T. Takubo, H. Yamada, T. Inoue, K. Nagaoka and Y. Takita, *J. Colloid Interface Sci.*, 2009, **332**, 136–144; (e) D. Kashiwagi, A. Takai, T. Takubo, K. Nagaoka, T. Inoue and Y. Takita, *Ind. Eng. Chem. Res.*, 2009, **48**, 632–640; (f) Y. Zhang, Y. Li, Z. Cui, D. Chen and X. Zhang, *AIP Adv.*, 2018, **8**, 55215.

10 (a) H. Deubner and F. Kraus, *Inorganics*, 2017, **5**, 68; (b) H. C. Cowen, F. Riding and W. Warhurst, *J. Chem. Soc.*, 1953, 4168–4169; (c) G. C. Demitras and A. G. MacDiarmid, *Inorg. Chem.*, 1964, **3**, 1198–1199.

11 M. Rueping, P. Nikolaienko, Y. Lebedev and A. Adams, *Green Chem.*, 2017, **19**, 2571–2575.

12 D. Sevenard, P. Kirsch, A. A. Kolomeitsev and G.-V. Rosenthaler, Patent DE10220901, 2004.

13 A. Taponard, T. Jarroson, L. Khrouz, M. Médebielle, J. Broggi and A. Tlili, *Angew. Chem., Int. Ed.*, 2022, DOI: [10.1002/anie.202204623](https://doi.org/10.1002/anie.202204623).

14 F. Buß, C. Mück-Lichtenfeld, P. Mehlmann and F. Dielmann, *Angew. Chem., Int. Ed.*, 2018, **57**, 4951–4955.

15 P. Tomar, T. Braun and E. Kemnitz, *Chem. Commun.*, 2018, **54**, 9753–9756.

16 S. Huang, Y. Wang, C. Hu and X. Yan, *Chem.: Asian J.*, 2021, **16**, 2687–2693.

17 (a) B. S. N. Huchenski and A. W. H. Speed, *Chem. Commun.*, 2021, **57**, 7128–7131; (b) R. F. Weitkamp, B. Neumann, H.-G. Stamm and B. Hoge, *Chem. – Eur. J.*, 2021, **27**, 6465–6478.

18 G. Iakobson, M. Pošta and P. Beier, *J. Fluorine Chem.*, 2018, **213**, 51–55.

19 D. J. Sheldon and M. R. Crimmin, *Chem. Commun.*, 2021, **57**, 7096–7099.

20 L. Zámostná and T. Braun, *Angew. Chem., Int. Ed.*, 2015, **54**, 10652–10656.

21 (a) L. Zámostná, T. Braun and B. Braun, *Angew. Chem., Int. Ed.*, 2014, **53**, 2745–2749; (b) P. Holze, B. Horn, C. Limberg, C. Matlachowski and S. Mebs, *Angew. Chem., Int. Ed.*, 2014, **53**, 2750–2753; (c) B. G. Harvey, A. M. Arif, A. Glöckner and R. D. Ernst, *Organometallics*, 2007, **26**, 2872–2879; (d) R. Basta, B. G. Harvey, A. M. Arif and R. D. Ernst, *J. Am. Chem. Soc.*, 2005, **127**, 11924–11925.

22 C. Berg, T. Braun, M. Ahrens, P. Wittwer and R. Herrmann, *Angew. Chem., Int. Ed.*, 2017, **56**, 4300–4304.

23 (a) X. Song, X. Liu, Z. Ye, J. He, R. Zhang and H. Hou, *J. Hazard. Mater.*, 2009, **168**, 493–500; (b) L. Huang, Y. Shen, W. Dong, R. Zhang, J. Zhang and H. Hou, *J. Hazard. Mater.*, 2008, **151**, 323–330; (c) L. Huang, D. Gu, L. Yang, L. Xia, R. Zhang and H. Hou, *J. Environ. Sci.*, 2008, **20**, 183–188; (d) L. Huang, W. Dong, R. Zhang and H. Hou, *Chemosphere*, 2007, **66**, 833–840.

24 D. Rombach and H.-A. Wagenknecht, *Angew. Chem., Int. Ed.*, 2020, **59**, 300–303.

25 D. Rombach and H.-A. Wagenknecht, *ChemCatChem*, 2018, **10**, 2955–2961.

26 T. A. McTeague and T. F. Jamison, *Angew. Chem., Int. Ed.*, 2016, **55**, 15072–15075.

27 S. Kim, Y. Khomutnyk, A. Bannykh and P. Nagorny, *Org. Lett.*, 2021, **23**, 190–194.

28 (a) S. Bouvet, B. Pégot, S. Sengmany, E. Le Gall, E. Léonel, A.-M. Goncalves and E. Magnier, *Beilstein J. Org. Chem.*, 2020, **16**, 2948–2953; (b) M. Govindan, R. Adam Gopal and I. S. Moon, *Chem. Eng. J.*, 2020, **382**, 122881; (c) Y. Li, A. Khurram and B. M. Gallant, *J. Phys. Chem. C*, 2018, **122**, 7128–7138.

29 (a) M. A. Wünsche, P. Mehlmann, T. Witteler, F. Buß, P. Rathmann and F. Dielmann, *Angew. Chem., Int. Ed.*, 2015, **54**, 11857–11860; (b) P. Mehlmann, C. Mück-Lichtenfeld, T. T. Y. Tan and F. Dielmann, *Chem. – Eur. J.*, 2017, **23**, 5929–5933.

30 (a) S. Ullrich, B. Kovačević, X. Xie and J. Sundermeyer, *Angew. Chem., Int. Ed.*, 2019, **58**, 10335–10339; (b) M. D. Böhme, T. Eder, M. B. Röthel, P. D. Dutschke, L. F. B. Wilm, E. Hahn and F. Dielmann, *Angew. Chem., Int. Ed.*, 2022, DOI: [10.1002/anie.202202190](https://doi.org/10.1002/anie.202202190); (c) F. Buß,

P. Mehlmann, C. Mück-Lichtenfeld, K. Bergander and F. Dielmann, *J. Am. Chem. Soc.*, 2016, **138**, 1840–1843; (d) F. Buß, P. Rotering, C. Mück-Lichtenfeld and F. Dielmann, *Dalton Trans.*, 2018, **47**, 10420–10424; (e) F. Buß, M. B. Röthel, J. A. Werra, P. Rotering, L. F. B. Wilms, C. G. Daniliuc, P. Löwe and F. Dielmann, *Chem. – Eur. J.*, 2022, **28**, e202104021; (f) P. Rotering, L. F. B. Wilms, J. A. Werra and F. Dielmann, *Chem. – Eur. J.*, 2020, **26**, 406–411.

31 M. L. Kaufman and C. E. Griffin, *Tetrahedron Lett.*, 1965, **12**, 767–772.

32 J. D. L. Horner, *Tetrahedron Lett.*, 1965, **12**, 763–767.

33 Y. Sakaguchi and H. Hayashi, *J. Phys. Chem. A*, 2004, **108**, 3421–3429.

34 Y. Sakaguchi and H. Hayashi, *Chem. Phys. Lett.*, 1995, **245**, 591–597.

35 (a) S. Yasui, Y. Ogawa, K. Shioji, M. Mishima and S. Yamazaki, *Bull. Chem. Soc. Jpn.*, 2014, **87**, 988–996; (b) S. Yasui, M. M. R. Badal, S. Kobayashi and M. Mishima, *Chem. Lett.*, 2013, **42**, 866–868; (c) S. Yasui, Y. Ogawa, K. Shioji and S. Yamazaki, *Chem. Lett.*, 2013, **42**, 1478–1480.

36 T. Yanai, D. P. Tew and N. C. Handy, *Chem. Phys. Lett.*, 2004, **393**, 51–57.

37 F. Weigend and R. Ahlrichs, *Phys. Chem. Chem. Phys.*, 2005, **7**, 3297–3305.

38 (a) C. B. Caputo, D. Winkelhaus, R. Dobrovetsky, L. J. Hounjet and D. W. Stephan, *Dalton Trans.*, 2015, **44**, 12256–12264; (b) J. Möbus, T. vom Stein and D. W. Stephan, *Chem. Commun.*, 2016, **52**, 6387–6390; (c) S. Postle, V. Podgorny and D. W. Stephan, *Dalton Trans.*, 2016, **45**, 14651–14657; (d) J. M. Bayne, M. H. Holthausen and D. W. Stephan, *Dalton Trans.*, 2016, **45**, 5949–5957; (e) M. H. Holthausen, R. R. Hiranandani and D. W. Stephan, *Chem. Sci.*, 2015, **6**, 2016–2021; (f) M. H. Holthausen, M. Mehta and D. W. Stephan, *Angew. Chem., Int. Ed.*, 2014, **53**, 6538–6541; (g) M. Mehta, M. H. Holthausen, I. Mallov, M. Pérez, Z.-W. Qu, S. Grimme and D. W. Stephan, *Angew. Chem., Int. Ed.*, 2015, **54**, 8250–8254; (h) M. Tress, E. U. Mapesa, W. Kossack, W. K. Kipnusu, M. Reiche and F. Kremer, *Science*, 2013, **341**, 1371–1374.

39 L. J. Hounjet, C. B. Caputo and D. W. Stephan, *Angew. Chem., Int. Ed.*, 2012, **51**, 4714–4717.

40 (a) W. C. Firth, S. Frank, M. Garber and V. P. Wystrach, *Inorg. Chem.*, 1965, **4**, 765; (b) W. C. Smith, *J. Am. Chem. Soc.*, 1960, **82**, 6176; (c) K. M. Doxsee, E. M. Hanawalt and T. J. R. Weakley, *Inorg. Chem.*, 1992, **31**, 4420.

41 (a) D. Bornemann, C. R. Pitts, L. Wettstein, F. Brüning, S. Küng, L. Guan, N. Trapp, H. Grützmacher and A. Togni, *Angew. Chem., Int. Ed.*, 2020, **59**, 22790–22795; (b) D. Bornemann, F. Brüning, N. Bartalucci, L. Wettstein and C. R. Pitts, *Helv. Chim. Acta*, 2021, **104**, DOI: [10.1002/hlca.202000218](https://doi.org/10.1002/hlca.202000218).

42 (a) J. Eljo, M. Carle and G. Murphy, *Synlett*, 2017, 2871–2875; (b) Z. Yang and X. Shen, in *Fluorination*, ed. J. Hu and T. Umemoto, Springer Singapore, Singapore, 2018, pp. 1–7; (c) Y. Kobaqashi and C. Akashi, *Chem. Pharm. Bull.*, 1968, **16**, 1009.

43 G. A. Olah, M. Nojima and I. Kerekes, *Synthesis*, 1973, 487.

44 O. Cohen, R. Sasson and S. Rozen, *J. Fluorine Chem.*, 2006, **127**, 433–436.

45 G. A. Olah, M. Nojima and I. Kerekes, *J. Am. Chem. Soc.*, 1974, **96**, 925.

46 T. Scattolin, K. Deckers and F. Schoenebeck, *Org. Lett.*, 2017, **19**, 5740–5743.

47 (a) G. S. Lal, G. P. Pez, R. J. Pesaresi, F. M. Prozonic and H. Cheng, *J. Org. Chem.*, 1999, **64**, 7048–7054; (b) F. Beaulieu, L.-P. Beauregard, G. Courchesne, M. Couturier, F. LaFlamme and A. L'Heureux, *Org. Lett.*, 2009, **11**, 5050–5053; (c) C. Kaduk, H. Wenschuh, M. Beyermann, K. Forner, L. A. Carpino and M. Bienert, *Lett. Pept. Sci.*, 1996, **2**, 285–288; (d) A. L'Heureux, F. Beaulieu, C. Bennett, D. R. Bill, S. Clayton, F. LaFlamme, M. Mirmehrabi, S. Tadayon, D. Tovell and M. Couturier, *J. Org. Chem.*, 2010, **75**, 3401–3411.

48 S. B. Munoz, H. Dang, X. Ispizua-Rodriguez, T. Mathew and G. K. S. Prakash, *Org. Lett.*, 2019, **21**, 1659–1663.

49 J. K. Ruff, W. J. Schlientz, R. E. Dessy, J. M. Malm, G. R. Dobson and M. N. Memering, *Inorg. Synth.*, 1974, 84–90.

50 A. Rajput, M. Soni and B. Chakraborty, *ChemElectroChem*, 2022, DOI: [10.1002/celec.202101658](https://doi.org/10.1002/celec.202101658).

51 E. Podyacheva, E. Kuchuk and D. Chusov, *Tetrahedron Lett.*, 2019, **60**, 575–582.

52 B. Chakraborty, P. W. Menezes and M. Driess, *J. Am. Chem. Soc.*, 2020, **142**, 14772–14788.

53 (a) O. M. Demchuk, W. Świerczyńska, K. Dziuba, S. Frynas, A. Flis and K. M. Pietrusiewicz, *Phosphorus, Sulfur Silicon Relat. Elem.*, 2017, **192**, 64–68; (b) A. J. Stepen, M. Bursch, S. Grimme, D. W. Stephan and J. Paradies, *Angew. Chem., Int. Ed.*, 2018, **57**, 15253–15256.